

## Growth Kinetics of Amyloid-like Fibrils Derived from Individual Subunits of Soy $\beta$ -Conglycinin

Jin-Mei Wang,<sup>†</sup> Xiao-Quan Yang,<sup>\*,†</sup> Shou-Wei Yin,<sup>†</sup> De-Bao Yuan,<sup>‡</sup> Ning Xia,<sup>†,§</sup> and Jun-Ru Qi<sup>†</sup>

<sup>†</sup>Department of Food Science and Technology, South China University of Technology, Guangzhou 510640, People's Republic of China

<sup>‡</sup>Institute of Banana and Plantain, Chinese Academy of Tropical Agricultural Sciences, Haikou 570102, People's Republic of China

<sup>§</sup>School of Light Industry and Food Engineering, Guangxi University, Nanning 530004, People's Republic of China

**ABSTRACT:** The amyloid-like fibrillation of soy  $\beta$ -conglycinin subunits ( $\alpha$ ,  $\alpha'$ , and  $\beta$ ) upon heating (0–20 h) at 85 °C and pH 2.0 was characterized using dynamic light scattering, circular dichroism (CD), binding to amyloid dyes (Thioflavin T and Congo red), and atomic force microscopy. The fibrillation of all three subunits was accompanied by progressive polypeptide hydrolysis. The hydrolysis behaviors, fibrillation kinetics, and morphologies of amyloid-like fibrils considerably varied among  $\alpha$ ,  $\alpha'$ , and  $\beta$  subunits. Faster hydrolysis rates and special fragments were observed for the  $\alpha$  and  $\alpha'$  subunits compared to the  $\beta$  subunit. However, the order of the fibrillation rate and capacity to form  $\beta$ -sheets was  $\alpha' > \beta > \alpha$ , as evidenced by CD and Thioflavin T data. Moreover, sequential growth of twisted screw-structure fibrils, leading to macroscopic fibrils with distinct morphological characteristics, was observed for  $\beta$ -conglycinin and individual subunits. The different fibrillation kinetics and morphologies of  $\alpha$ ,  $\alpha'$ , and  $\beta$  subunits appear to be associated with the differences in the amino acid composition and typical sequence of peptides. Besides, the disruption of ordered structure of fibrils occurred upon further heating (6–20 h) due to extensive hydrolysis. These results would suggest that all subunits are involved in the fibrillation of  $\beta$ -conglycinin, following multiple steps including polypeptide hydrolysis, assembly to amyloid structure, and growth into macroscopic fibrils with a fibril shaving process.

**KEYWORDS:**  $\beta$ -conglycinin, individual subunits, polypeptide hydrolysis, conformational changes, assembly, amyloid fibril

### INTRODUCTION

Fibrillar aggregates of food proteins, especially whey protein and  $\beta$ -lactoglobulin, have attracted increasing attention owing to their potential application in food products, for example, as effective thickeners and gelling ingredients.<sup>1</sup> The concept of using food protein fibrils as microcapsules has also been established.<sup>2,3</sup> Generally, the formation of amyloid fibril with extensive  $\beta$ -sheet structure appears to be a generic property of polypeptide chains. With respect to some globular proteins, this process is readily triggered under conditions that promote their partial unfolding, particularly at low pH and high temperature.<sup>4</sup> Both whey proteins and  $\beta$ -lactoglobulin can aggregate into long semiflexible fibrils with contour lengths of 1–10  $\mu\text{m}$  and thicknesses of a few nanometers after heating at low pH.<sup>5,6</sup>

To tune the properties of amyloid fibrils derived from globular proteins, considerable attention has been directed to the growth kinetics of fibrils. It is widely believed that the formation of fibrils is a multistep process. Protein monomer rapidly converts into weakly associated aggregates and subsequently undergoes a conformational rearrangement into more organized protofibrils, which elongate in the growth phase.<sup>5,7,8</sup> The effects of incubation conditions on fibril formation of globular proteins, including protein concentration,<sup>9</sup> ionic strength,<sup>10</sup> and shear treatment,<sup>6</sup> have been investigated in detail. Recently, evidence has shifted some of the focus to the fibril component and the influence of protein hydrolysis on the formation of amyloid fibril.<sup>11–15</sup> The  $\beta$ -lactoglobulin fibrils formed by heating at pH 2.0 are composed of a part of peptides and not formed from intact monomers.<sup>11–13</sup> Furthermore, Akkermans et al.<sup>11</sup> reported that hydrophobic peptides with low charges were frequently present in these fibrils,

and a high capacity to form  $\beta$ -sheets was also speculated to be related to the presence of specific regions in the fibrils. It has been shown that protein hydrolysis affects the formation of amyloid fibrils derived from lysozyme and  $\beta$ -lactoglobulin at low pH and elevated temperature.<sup>14,15</sup> In fact, for other proteins, the protein sequence and amino acid composition indeed have an important influence on the capacity and rate of certain regions to form amyloid fibrils.<sup>16,17</sup>

Compared with whey proteins, fibril formation of plant proteins is less recognized due to their structural complexity. In the previous work, the formation of heat-induced amyloid-like fibrils of phaseolin has been confirmed.<sup>18</sup> Both soy protein isolate and glycinin could also convert to fibrillar aggregates with contour lengths of approximately 1  $\mu\text{m}$  and thicknesses of a few nanometers when heated at pH 2.0 and 85 °C.<sup>19</sup> Glycinin fibrils exhibit excellent properties (e.g., flow properties), which can be comparable to those of fibrils from  $\beta$ -lactoglobulin. Recently, it has been reported that soy  $\beta$ -conglycinin exhibits a higher capacity to form amyloid fibrils than glycinin, with lower width at half-heights and higher coil periodicity. The processes of soy protein fibrillation are accompanied by conformational changes and hydrolysis.<sup>20</sup>  $\beta$ -Conglycinin, as one of the major globulins in soy proteins, is a trimer having a molecular weight of approximately 180 kDa and is composed of three major subunits:  $\alpha$  (67 kDa),  $\alpha'$  (71 kDa), and  $\beta$  (50 kDa). The  $\alpha$  and  $\alpha'$  subunits consist of extension regions and core regions, whereas the  $\beta$

**Received:** June 28, 2011

**Revised:** September 15, 2011

**Accepted:** September 15, 2011

**Published:** September 15, 2011

subunit is composed of only core regions.<sup>21</sup> The extension regions of these subunits exhibit 57% sequence identity, and the core regions show high absolute homologies (90, 76, and 75% between  $\alpha$  and  $\alpha'$ , between  $\alpha$  and  $\beta$ , and between  $\alpha'$  and  $\beta$ , respectively).<sup>21</sup> Moreover, compared to the  $\beta$  subunit, the  $\alpha$  and  $\alpha'$  subunits display lower hydrophobicity due to the richness of acidic amino acids in the extension regions.<sup>21</sup>

In our laboratory, the  $\alpha$ ,  $\alpha'$ , and  $\beta$  subunits have been successfully isolated from  $\beta$ -conglycinin.<sup>22</sup> The main objective of the present study was to characterize the formation processes of amyloid-like fibrils derived from individual subunits ( $\alpha$ ,  $\alpha'$ , and  $\beta$ ) at pH 2.0 and 85 °C using dynamic light scattering (DLS), circular dichroism (CD), and binding to amyloid dyes (Thioflavin T and Congo red) as well as atomic force microscopy (AFM). Sodium dodecyl sulfate–polyacrylamide gel electrophoresis (SDS-PAGE) was used to monitor the polypeptide hydrolysis kinetics of  $\beta$ -conglycinin and its subunits. The roles of individual subunits and the possible steps involved in fibril formation of  $\beta$ -conglycinin were also discussed.

## MATERIALS AND METHODS

**Materials.** Defatted soy seed flour was provided by Shandong Yuwang Industrial and Commercial Co., Ltd. (Shandong, China). The protein content of soy flour was  $47.47 \pm 2.10\%$  (determined by micro-Kjeldahl method,  $N \times 5.71$ , wet basis). The resins (DEAE-Sepharose Fast Flow, Chelating Sepharose Fast Flow) and two columns ( $4.5 \times 25$  cm,  $6 \times 35$  cm) were purchased from Pharmacia Co. (Uppsala, Sweden). Thioflavin T (Th T) and Congo red (CR) were purchased from Sigma-Aldrich (St. Louis, MO). All other reagents and chemicals were of analytical grade.

**Preparation of  $\beta$ -Conglycinin and Isolation of Subunits ( $\alpha$ ,  $\alpha'$ , and  $\beta$ ).** Soybean  $\beta$ -conglycinin was prepared from soy flour according to the method of Nagano et al.<sup>23</sup> The protein content of  $\beta$ -conglycinin was  $86.89 \pm 1.46\%$  (determined by micro-Kjeldahl method,  $N \times 5.71$ , wet basis). The  $\alpha$ ,  $\alpha'$ , and  $\beta$  subunits were isolated according to the method of Yuan et al.<sup>22</sup>  $\beta$ -Conglycinin in the standard buffer (0.05 M borate buffer, containing 6.0 M urea, pH 9.0) was loaded on the column ( $6 \times 35$  cm) previously equilibrated with the same buffer. Elution was performed with the standard buffer containing NaCl in a step gradient of 0–0.3 M at a flow rate of 5 mL/min. The purified  $\beta$  subunit and the mixtures of  $\alpha$  and  $\alpha'$  subunits were obtained by collecting specific protein fractions, followed by dialysis against distilled water at 4 °C and lyophilization. Then the mixtures of  $\alpha$  and  $\alpha'$  subunits were redissolved in 0.05 M Tris-HCl buffer (pH 7.0, containing 0.5 M NaCl and 6 M urea) and loaded onto the IMAC column ( $4.5 \times 25$  cm) coupled with  $\text{Cu}^{2+}$ . The column was thoroughly washed with the same buffer to elute the unbound fraction. Elution was performed with the same buffer containing imidazole in a linear gradient of 0–0.1 M at a flow rate of 5 mL/min. Purified  $\alpha$  and  $\alpha'$  subunits were collected, dialyzed against distilled water at 4 °C, and then lyophilized.

**Heat-Induced Aggregation at pH 2.0.** Lyophilized  $\beta$ -conglycinin and its subunits ( $\alpha$ ,  $\alpha'$ , and  $\beta$ ) were dissolved in distilled water for 2 h at room temperature, and then the pH of protein solutions was accurately adjusted to 2.0 with 2 M HCl. Protein solutions were hydrated at 4 °C overnight before heat treatment. The protein dispersions were centrifuged at 10000g for 20 min in a CR22G centrifuge (Hitachi Co., Japan). The protein concentrations of supernatant were determined according to Lowry's method<sup>24</sup> using bovine serum albumin (BSA) as standard and adjusted to 10 mg/mL. All samples were placed in hermetic bottles and then heated at 85 °C for specific periods of time. After heat treatment, the samples were immediately cooled in an ice bath for further analysis.

**Sodium Dodecyl Sulfate–Polyacrylamide Gel Electrophoresis.** A time course analysis of the molecular composition of amyloid fibrils from  $\beta$ -conglycinin and its subunits was assessed by SDS-PAGE. Proteins (40  $\mu\text{L}$ ) incubated at different time points were quickly mixed with SDS sample buffer (120  $\mu\text{L}$ , 150 mM Tris-HCl, 20% glycerol, 1% SDS, 4% 2-mercaptoethanol, pH 6.8) and heated at 95 °C for 5 min. SDS-PAGE was performed on a discontinuous buffered system according to the method of Laemmli<sup>25</sup> using 12.5% separating gel and 5% stacking gel. The gel was stained using Coomassie brilliant blue (R-250) stain solution (45% methanol, 10% acetic acid, and 0.25% R-250) and destained in methanol–water solution containing 10% acetic acid (methanol/acetic acid/water = 1:1:8, v/v/v).

**Dynamic Light Scattering.** The heated protein samples at different points were diluted to 1 mg/mL with distilled water (pH 2.0) filtered through a 0.22  $\mu\text{m}$  filter (Millipore, Fisher Scientific) before measurement. The sample was placed in a 1 cm  $\times$  1 cm cuvette. DLS analysis was performed at a fixed angle of 173° using a Zetasizer Nano-ZS instrument (Malvern Instruments, Worcestershire, U.K.) equipped with a 4 mW He–Ne laser (633 nm wavelength) at 25 °C. The appropriate viscosity and refractive index parameters for each solution were set. The time-average (or “total”) intensity (kcps) of the scattered light at different points was collected to obtain qualitative information about the time required for the formation of aggregates using Dispersion Technology Software (DTS) (V4.20).<sup>26</sup>

**Circular Dichroism Spectroscopy.** Far-UV CD spectra of proteins heated at different time points were obtained using an MOS-450 spectropolarimeter (Bio-Logic Science Instruments, Grenoble, France) in cylindrical cells (2 mm path length) at 25 °C. The following parameters were used: step resolution, 0.5 nm; acquisition duration, 1 s; bandwidth, 5.0 nm; sensitivity, 100 mdeg. The protein dispersions were diluted to 0.1 mg/mL with distilled water (pH 2.0). The spectra in the far-UV (190–250 nm) region were an average of six scans. The spectrum of distilled water (pH 2.0) as a control was subtracted from spectra of the samples. CD measurements were expressed as mean residue ellipticity in  $\text{deg cm}^2 \text{dmol}^{-1}$ .

**Thioflavin T Fluorescence Assay.** A Th T stock solution was prepared at a concentration of 0.8 mg/mL (2.5 mM) in phosphate buffer (5 mM potassium phosphate containing 150 mM NaCl, pH 7.4) and filtered through a 0.22  $\mu\text{m}$  filter to remove undissolved Th T before use.<sup>27</sup> This stock solution was diluted 50-fold in the phosphate buffer to generate the working solution (50  $\mu\text{M}$ ). Aliquots (40  $\mu\text{L}$ ) of samples were mixed with 4 mL working solution and then allowed to bind the Th T for 2 min. The fluorescence intensity of the heated protein–Th T dye mixtures was measured at 440 nm (excitation, slit width 5 nm) and 482 nm (emission, slit width 5 nm) using an F7000 fluorescence spectrophotometer (Hitachi Co., Japan). The fluorescence intensity of the Th T working solution as a control was subtracted from the fluorescence intensity of protein samples.

**Curve-Fitting Program.** The aggregation kinetic in the initial stage of amyloid-like fibril formation was obtained by monitoring the changes in mean residue ellipticity at 216 nm by far-UV CD and Th T fluorescence intensity. The kinetics of amyloid-like aggregation were fit to a single-exponential rate equation

$$y = q + A \exp(-kt) \quad (1)$$

where  $A$  is the total change in mean residue ellipticity or fluorescence intensity during the exponential phase and  $k$  is the apparent rate constant.<sup>28</sup>

**Congo Red Binding Assay.** The CR stock solution was prepared by dissolving the dye in potassium phosphate buffer (5 mM potassium phosphate containing 150 mM NaCl, pH 7.4) at a concentration of 0.7 mg/mL (1 mM) and filtering through a 0.22  $\mu\text{m}$  filter.<sup>27</sup> The protein samples were mixed with a solution of CR to yield a final CR concentration of 50  $\mu\text{M}$  and a final protein concentration of 75  $\mu\text{g/mL}$  and then incubated at room temperature for at

least 30 min. Absorption spectra were recorded from 400 to 600 nm on a UV2300 spectrophotometer (Techcomp, China). The differential spectra were obtained by subtracting the blank spectrum (CR dye alone) from the sample spectra.

**Atomic Force Microscopy.** AFM images were recorded at room temperature in tapping mode at a drive frequency of approximately 320 kHz, and the scan rate was 1.0 Hz using a MultiMode SPM microscope equipped with a Nanoscope IIIa Controller (Digital Instruments, Veeco, Santa Barbara, CA). PointProbe NCHR silicon tips of 125  $\mu\text{m}$  in length with a spring constant of 42 N/m were purchased from NanoWorld

(Arrow NC cantilevers, Nanoworld, Switzerland). Typical resonant frequencies of these tips were about 290 kHz. Aliquots (2  $\mu\text{L}$ ) of heated protein dispersions (diluted to 10  $\mu\text{g}/\text{mL}$  with distilled water filtered through a 0.22  $\mu\text{m}$  filter, pH 2.0) were placed on a freshly cleaved mica disk and air-dried for 10 min at ambient temperature. Control samples (freshly cleaved mica) were detected to exclude possible artifacts. Images were analyzed using Digital Nanoscope software (version 5.30r3, Digital Instruments, Veeco).

**Statistics.** Unless specified otherwise, three independent trials were performed, each with a new batch of sample preparation. All of the tests were carried out in duplicate or triplicate, and an analysis of variance (ANOVA) of the data was performed using the SPSS 13.0 statistical analysis system. A least significant difference (LSD) test with a confidence interval of 95% was used to compare the means.

## RESULTS AND DISCUSSION

**Protein Hydrolysis As Assessed by Sodium Dodecyl Sulfate–Polyacrylamide Gel Electrophoresis.** The  $\alpha$ ,  $\alpha'$ , and  $\beta$  subunits with >80% protein purity were successfully isolated from  $\beta$ -conglycinin, as identified by SDS-PAGE (Figure 1). The molecular weights of the  $\alpha$ ,  $\alpha'$ , and  $\beta$  subunits were calculated to be about 67.0, 71.0, and 50.0 kDa, respectively. Figure 2 shows a time course analysis of polypeptide hydrolysis of  $\beta$ -conglycinin and individual subunits. The typical polypeptide bands were observed for all unheated samples. Besides the major bands, new bands with lower molecular mass (MW) were found in the  $\alpha$  and  $\alpha'$  subunits before heat treatment (Figure 2B, b2; Figure 2C, b1),

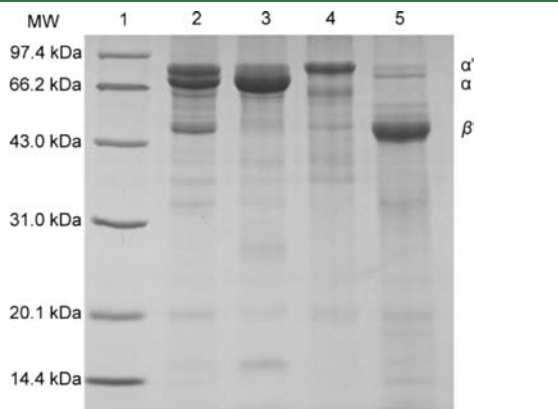


**Figure 1.** SDS-PAGE profile for isolated subunits of  $\beta$ -conglycinin. Lanes: 1, protein makers; 2,  $\beta$ -conglycinin; 3,  $\alpha$  subunit; 4,  $\alpha'$  subunit; 5,  $\beta$  subunit.

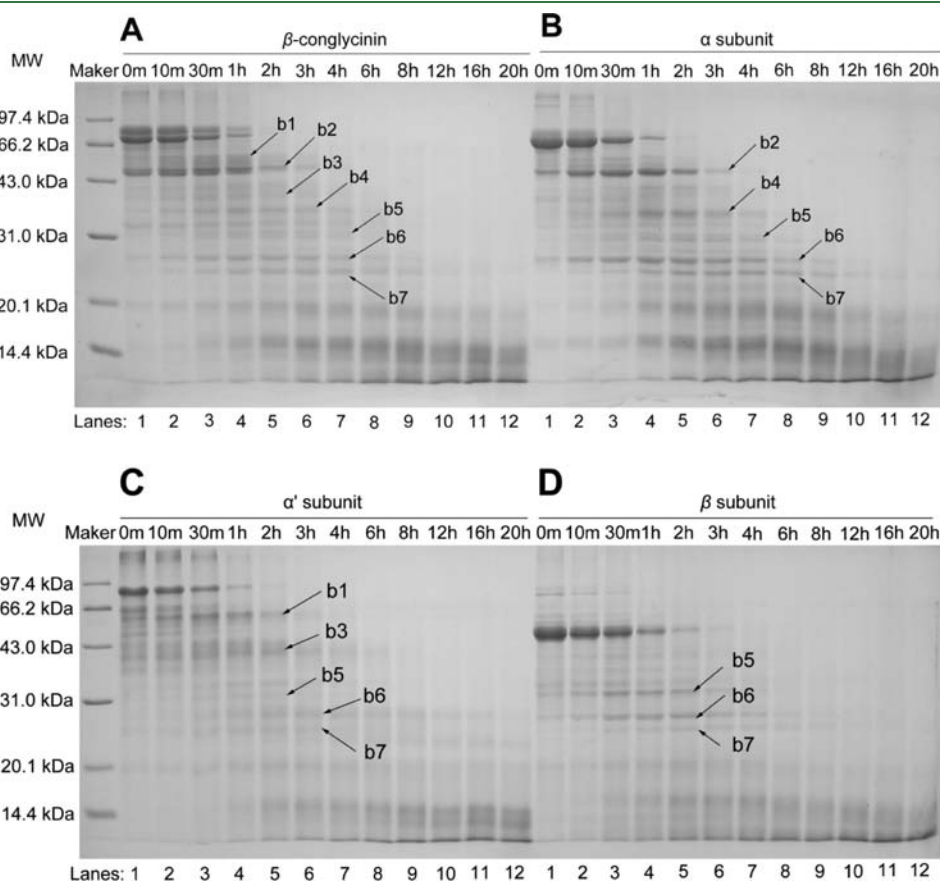


**Figure 2.** Hydrolysis kinetics during fibril formation of  $\beta$ -conglycinin (A) and  $\alpha$  (B),  $\alpha'$  (C), and  $\beta$  (D) subunits monitored by reducing SDS-PAGE. Molecular mass markers (in kDa) are shown on the left-hand side of the gels.

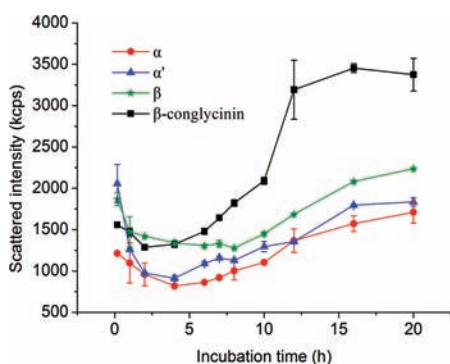


**Figure 3.** Temporal evolution of the scattered intensity of  $\beta$ -conglycinin and  $\alpha$ ,  $\alpha'$ , and  $\beta$  subunits at pH 2.0 and 85 °C monitored by DLS.

which might be released fragments of subunits at acidic pH. Upon heating, as expected, the density of the major bands progressively decreased for all samples, and some bands (e.g., b3–7) with smaller molecular mass simultaneously appeared, which further hydrolyzed into peptides with MW < 20 kDa after extended incubation. Previous papers have shown that  $\beta$ -conglycinin undergoes a fragmentation process at pH 2.0 and 80 °C, which promotes the formation of amyloid-like fibrils.<sup>20</sup>

Overall, the hydrolysis fragments of  $\beta$ -conglycinin appeared to be a mixture of peptides released from three individual subunits (Figure 2A, b1–7), clearly indicating that the separation process of subunits had no influence on their hydrolysis behaviors at acid condition, compared with the hydrolysis of a trimer. The protein hydrolysis behaviors considerably varied among various subunits based on the differences in the molecular mass of fragments and the kinetics of fragmentation. In the initial of hydrolysis, it seemed that the  $\alpha$  and  $\alpha'$  subunits disappeared in 2 h (Figure 2B,C, lanes 2–5), whereas the  $\beta$  subunit was completely disrupted in 4 h (Figure 2D, lanes 2–7). These phenomena suggest that the  $\alpha$  and  $\alpha'$  subunits may be more easily hydrolyzed than the  $\beta$  subunit (Figure 2). Tang et al.<sup>20</sup> proposed a similar viewpoint based on the hydrolysis of  $\beta$ -conglycinin. However, interestingly, heated  $\alpha$  subunit showed a fragment with a molecular mass of 50.0 kDa (Figure 2B, b2), which was similar to the  $\beta$  subunit. Moreover, the intensity of this band gradually increased during initial heating (0–1 h) and then decreased until disappearing at 4 h, which probably guided researchers to make an inaccurate deduction based on the hydrolysis of a trimer. Thus, the results of individual subunit hydrolysis further support the viewpoint of easier disruption of the  $\alpha$  and  $\alpha'$  subunits. This may be explained by the difference in amino acid composition of the subunits. That is, the  $\alpha$  and  $\alpha'$  subunits are rich in charged acidic amino acids, especially aspartic acid residues, which can be preferentially hydrolyzed under acid pH when the  $\beta$ -carboxyl group is protonated.<sup>29</sup> This is further confirmed by cleavage of the peptide bonds before or after Asp residues for  $\beta$ -lactoglobulin.<sup>11</sup>

On the other hand, almost all fragments appearing in the  $\beta$  subunit (Figure 2D) were also observed in the  $\alpha$  and  $\alpha'$  subunits (Figure 2B,C, b5–7). However, the typical bands were found in the  $\alpha$  and  $\alpha'$  subunits (Figure 2B,C, b1–4). These various hydrolysis behaviors among the  $\alpha$ ,  $\alpha'$ , and  $\beta$  subunits may be related to the differences in the heat-induced cleavage sites due to their specific amino acid sequences. Because of the structural characteristics of three subunits, such as high homology of amino acid sequences among the core regions and the

richness of acidic amino acids in the extension regions of the  $\alpha$  and  $\alpha'$  subunits,<sup>21</sup> it could be speculated that the extension regions of the  $\alpha$  and  $\alpha'$  subunits may be responsible for the different hydrolysis behaviors.

**Aggregates Formation As Assessed by Dynamic Light Scattering.** DLS as a quantitative technique has been proved to be a sensitive and powerful method in monitoring the formation of aggregates and the growth of fibrils. The scattering intensity of an aggregate is proportional to the mass and number of particles.<sup>30</sup> Figure 3 shows the temporal evolution of the scattering intensity of  $\beta$ -conglycinin and its subunits. In all cases, there were similar changes in scattering intensity. In the initial stage, heating resulted in a decrease of scattering intensity, which might be attributed to the fact that  $\beta$ -conglycinin and its subunits converted into some fragments due to the progressive polypeptide hydrolysis. The increases of scattering intensity were distinctly observed upon further heating, although further hydrolysis sequentially occurred, as evidenced by SDS-PAGE (Figure 2). The changes in the apparent hydrodynamic radii for all samples are in accordance with the scattering intensity (data not shown). Tang et al.<sup>20</sup> reported the fibril formation of  $\beta$ -conglycinin by heating at pH 2.0. If so, this increase indicates the formation of aggregates or fibril using these peptides as building blocks. It has been reported that the  $\beta$ -lactoglobulin fibrils formed at pH 2.0 are composed of peptides and that the formation of peptides precedes their incorporation into the fibrils.<sup>11,15</sup>

It is noteworthy that the lowest scattering intensity of  $\beta$ -conglycinin and its subunits appeared at different incubation times, suggesting that all samples showed various transition rates from peptides to larger aggregates.  $\beta$ -Conglycinin exhibited the fastest transition of the scattering intensity (at 2 h), and the increase rate gradually decreased in the later stage of aggregation (12 h). By contrast, for the individual subunits, the rates and strengths of increase in scattering intensity were all lower than those of  $\beta$ -conglycinin, and no plateau was observed even after heating for 20 h. These results indicate that all individual subunits may be involved in the fibril formation of  $\beta$ -conglycinin, accompanied by cooperation with each other, but still not rejecting the influence of urea-induced denaturation on the capacity to form fibrils during the isolated process of subunits.

Considerable various changes in scattering intensity were observed among the three subunits. The  $\alpha$  and  $\alpha'$  subunits showed lower scattering intensity than the  $\beta$  subunit in the initial heating (0–4 h). This is probably a result of the higher decreases in the mass of fragments by disruption of the extension region of the  $\alpha$  and  $\alpha'$  subunits. The extension regions are considered to form a projection on the surface of the core region and contribute to the molecular dimension.<sup>21</sup> These results also further support the hypothesis that the  $\alpha$  and  $\alpha'$  subunits are more easily disrupted than the  $\beta$  subunit, as observed by SDS-PAGE (Figure 2). In addition, the  $\beta$  subunit exhibited a slower transition rate (8 h) and a higher scattering intensity at 20 h than the  $\alpha$  and  $\alpha'$  subunits (Figure 3). As a result, it is speculated that various subunits possibly play different roles in the fibril formation of  $\beta$ -conglycinin. The  $\beta$  subunit may be in charge of the increase in the amount of conversion from peptides to aggregates. In compliance with the polypeptide hydrolysis (Figure 2), differences in hydrolysis sites could largely account for these differences in aggregation behaviors.

**Structural Transition during Amyloid-like Fibril Formation.** More details in structural transition are desired to better delineate the steps involved in the fibril formation of  $\beta$ -conglycinin and

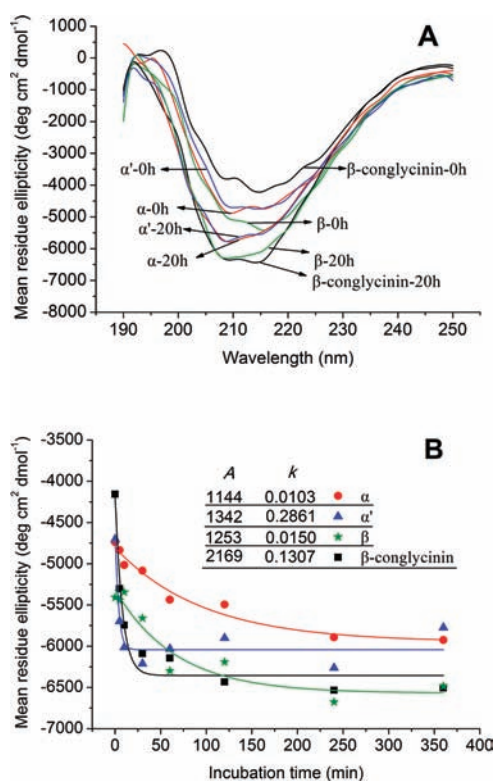


**Figure 4.** (A) Far-UV CD spectra of amyloid-like fibrils from  $\beta$ -conglycinin and  $\alpha$ ,  $\alpha'$ , and  $\beta$  subunits. (B) Mean residue ellipticity (at 216 nm) monitored kinetics of the amyloid-like fibril formation. Mean residue ellipticity at 216 nm versus time (0–6 h) is well described as a single exponential.

subunits, because the DLS approach cannot gain information about the common amyloid traits (e.g., staining properties). Molecular conformational changes, especially the formation of ordered  $\beta$ -type secondary structure, are usually correlated with the formation of amyloid fibrils. In addition, amyloid dyes such as Th T and CR have been widely used to identify the presence of amyloid structure.<sup>27</sup>

**Circular Dichroism Assay.** The secondary structural changes of unheated and heated samples were characterized using far-UV CD spectra, as shown in Figure 4A. The spectra for unheated  $\alpha$  and  $\alpha'$  subunits showed significant dips at 208 nm, whereas the spectra for unheated  $\beta$ -conglycinin and  $\beta$  subunit exhibited significant dips at 216 nm, indicating conformational differences among various samples (Figure 4A). Heating for 0–20 h at pH 2.0 led to remarkable increases in the magnitude of the negative bands for all samples, particularly for  $\beta$ -conglycinin, suggesting the formation of more ordered structures (Figure 4A). In all cases, the prominent conformational changes occurred during initial heating (e.g., <6 h), and then the transition rates slowed upon further heating (6–20 h) (data not shown).

The mean residue ellipticity at 216 nm, indicative of  $\beta$ -type secondary structure, was thereby used to quantitatively monitor the initial kinetics of amyloid-like fibril formation. Figure 4B presents the changes of mean residue ellipticity as a function of incubation time. Single-exponential fitting was used to obtain the kinetic parameters (see eq 1), because no obvious lag phase was visible for any of the samples. The apparent rate constant ( $k$ ) and amplitude ( $A$ ) of conformational changes considerably varied among  $\beta$ -conglycinin and the three subunits. The order of the

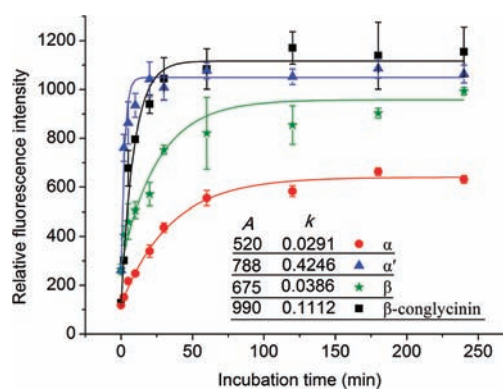


**Figure 5.** Th T fluorescence-monitored kinetics of amyloid-like fibril formation of  $\beta$ -conglycinin and  $\alpha$ ,  $\alpha'$ , and  $\beta$  subunits. Th T fluorescence intensity versus time (0–4 h) is well described as a single exponential.

total changes in mean residue ellipticity was  $\beta$ -conglycinin (2169) >  $\alpha'$  (1342) >  $\beta$  (1253) >  $\alpha$  (1144), whereas the order of the apparent rate constant was  $\alpha'$  (0.2861) >  $\beta$ -conglycinin (0.1307) >  $\beta$  (0.0150) >  $\alpha$  (0.0103). These results clearly suggest different capacities to form extensive  $\beta$ -sheets and fibrillation rates. Moreover, three subunits probably play different roles in the formation of amyloid-like structure by involving different pathways of fibrillation. In view of the protein sequence of three subunits (<http://www.ncbi.nlm.nih.gov/protein>, BAB64304.1, BAB64303.1, and BAB64306.1), the amino acid proline is rich in the extension regions of the  $\alpha$  and  $\alpha'$  subunits. Proline has been reported to be energetically unfavorable for the formation of  $\beta$ -sheets.<sup>31</sup> However, this information appears to be contradictory to the fact that the  $\alpha'$  subunit has the fastest rate and the highest capacity to form extensive  $\beta$ -sheets among three subunits (Figure 4B). Thus, we could properly not only speculate that the local complexity of amino acid sequences for various subunits probably interferes with the formation of amyloid-like fibrils but also infer that the extension regions of the  $\alpha$  and  $\alpha'$  subunits may be bound with the conformational transition.

It should be noted that the magnitude of the negative bands decreased in all samples when the incubation time was prolonged up to 20 h (data not shown). This finding is in agreement with previous results on  $\beta$ -lactoglobulin.<sup>12</sup> This may be attributed to the disruption of the ordered secondary structure by further hydrolysis of formed amyloid fibrils, which is called the “fibril shaving process” for other proteins.<sup>32</sup> Thus, it could be deduced that the growth of the amyloid-like fibrils also involves the disruption and reorganization of the ordered secondary structures.

**Thioflavin T and Congo Red Assays.** The growth kinetics of the amyloid fibrils from  $\beta$ -conglycinin and its subunits monitored by Th T fluorescence is shown in Figure 5. All unheated samples showed relatively low fluorescence intensity. In the initial stage, heating led to a sharp increase in fluorescence intensity before finally leveling off (about 1 h), suggesting that the transition of the amyloid fibrillar structures was completely finished within a short time. This result is well consistent with the changes in secondary conformation for all samples (Figure 4). Similar to the CD data, the fibril formation of  $\beta$ -conglycinin and subunits displayed single-exponential kinetics (Figure 5). In addition, the apparent rate constant and the total change in fluorescence intensity considerably varied among  $\beta$ -conglycinin and subunits (Figure 5). The order of apparent rate constant was

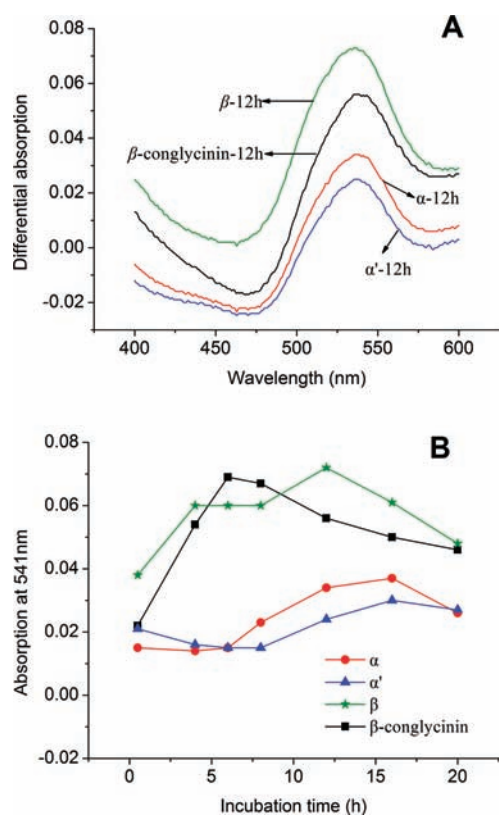


**Figure 6.** (A) CR spectroscopic profiles binding to amyloid-like fibrils derived from  $\beta$ -conglycinin and  $\alpha$ ,  $\alpha'$ , and  $\beta$  subunits by heating at pH 2.0 for 20 h. (B) Temporal evolution of CR absorption at 541 nm for heated samples.

$\alpha'$  (0.4246) >  $\beta$ -conglycinin (0.1112) >  $\beta$  (0.0386) >  $\alpha$  (0.0291), and the order of the total change in fluorescence intensity was  $\beta$ -conglycinin (990) >  $\alpha'$  (788) >  $\beta$  (675) >  $\alpha$  (520), indicating the different transition rates and capacities to form the amyloid structure binding to Th T. These observations are in a fairly good agreement with CD data (Figure 4B).

The samples heated for different incubation periods were subjected to the CR assay to determine the capacity of binding to this dye, as shown in Figure 6. The appearance of maximum absorption at approximately 520–540 nm in the differential spectra suggests the CR binding to the amyloid-like fibrils of  $\beta$ -conglycinin and its subunits (Figure 6A). However, considerable differences in absorption in all samples may indicate the different structural properties of formed amyloid fibrils. In addition, the CR dye binding was accompanied by a significant increase in absorption intensity when the incubation period was increased, whereas prolonged heating decreased their magnitudes (at 6, 16, 16, and 12 h for  $\beta$ -conglycinin and the  $\alpha$ ,  $\alpha'$ , and  $\beta$  subunits, respectively) (Figure 6B). These results probably suggest the decrease in amyloid structure during the later stage of amyloid fibril formation, consistent with CD data (Figure 4). The proper explanation is that, at this stage, the fibrils are further packed together, leading to the masking of binding sites for CR on the fibril's surface. Additionally, excessive hydrolysis may be another possible reason, as evidenced by SDS-PAGE (Figure 2).

**Sequential Growth of Aggregates As Monitored by Atomic Force Microscopy.** The morphological details of fibrils derived from  $\beta$ -conglycinin and its subunits were investigated

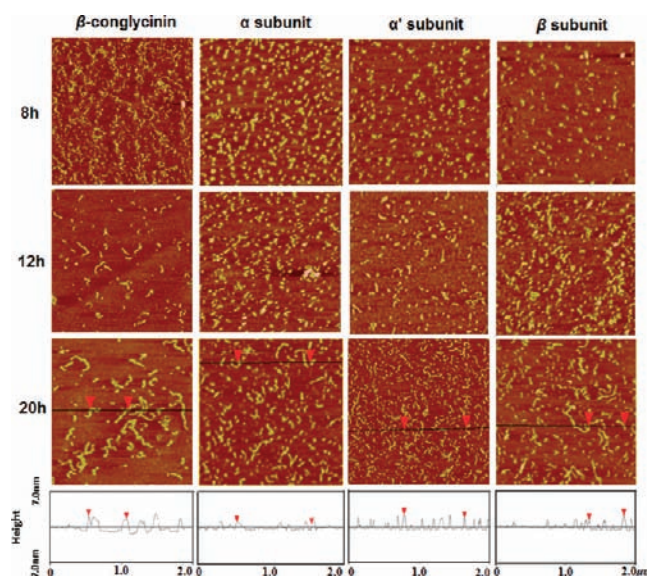


**Figure 7.** Tapping mode AFM height images of fibrils derived from  $\beta$ -conglycinin and  $\alpha$ ,  $\alpha'$ , and  $\beta$  subunits obtained at different incubation times. All of the images correspond to a sample area of  $2 \times 2 \mu\text{m}$ . The height profiles of the fibrils located at red lines (within the figures) are presented below the AFM images.

by AFM. Figure 7 shows the tapping mode AFM height images of fibrillar aggregates obtained by heating at  $85^\circ\text{C}$  for different incubation times (e.g., 8, 12, and 20 h). The heating induced the formation of flexible fibrils with periodic or twisted coil structure, and their contour lengths were highly dependent on heating time. The macroscopic fibrils or rod-like aggregates formed for  $\beta$ -conglycinin and subunits at 8 h of heating and their lengths gradually increased upon prolonged heating (8–20 h) (Figure 7).

At 20 h of heating,  $\beta$ -conglycinin and individual subunits converted into the worm-like fibrils with average lengths of  $\sim 800$  and  $\sim 300$  nm, respectively. However, the distribution of fibrils derived from  $\beta$ -conglycinin was more relatively regular than that of individual subunits, which contained a mixture of small particles/aggregates and fibrils. This result suggests that it is easier for  $\beta$ -conglycinin to form fibrils and that the growth rate of  $\beta$ -conglycinin fibril is much faster than that of individual subunits upon this incubation condition, which are in accordance with the DLS observations (Figure 3). On the other hand, all samples exhibited similar heights (approximately 2 nm) after heating for 20 h (Figure 7). However, the coil periodicity and the width at half-heights of formed fibrils varied considerably among  $\beta$ -conglycinin and its subunits (Table 1).  $\beta$ -Conglycinin fibrils presented a width at half-height of 50.0 nm and a coil periodicity of 43.0 nm, which were higher than those of the fibrils derived from individual subunits. Particularly, the  $\alpha'$  subunit showed the smallest width at half-height (28.3 nm) and coil periodicity (23.4 nm). These findings indicate that various individual subunits may undergo different pathways of thermal aggregation, leading to macroscopic fibrils with distinct morphological characteristics.

**General Discussion.** In this work, heating at pH 2.0 and  $85^\circ\text{C}$  led to fibril formation of  $\beta$ -conglycinin and  $\alpha$ ,  $\alpha'$ , and  $\beta$  subunits with twisted coil structure. Typical amyloid characteristics, such as extensive  $\beta$ -sheet structure and binding to amyloid dyes (Th T and CR), are also present in these fibrils (Figures 4–6). Moreover,  $\beta$ -conglycinin has a higher ability to form amyloid-like

**Table 1. Some Morphological Characteristics for Amyloid-like Fibrils of  $\beta$ -Conglycinin and Its Subunits ( $\alpha$ ,  $\alpha'$ , and  $\beta$ ) Heated at pH 2.0 for 20 h<sup>a</sup>**

sample	characteristics of the formed fibrils	
	width at half-height (nm)	coil periodicity (nm)
$\beta$ -conglycinin	50.0 $\pm$ 4.3 a	43.0 $\pm$ 4.5 a
$\alpha$	45.6 $\pm$ 5.9 a	27.3 $\pm$ 4.5 b
$\alpha'$	28.3 $\pm$ 2.0 b	23.4 $\pm$ 3.5 b
$\beta$	46.9 $\pm$ 4.9 a	29.0 $\pm$ 3.8 b

<sup>a</sup> The characteristics of the formed fibrils were obtained from the AFM images. Each data point is the mean and standard deviation of at least six determinations. Different letters in the same column indicate significant ( $p < 0.05$ ) differences among samples.

fibrils than the individual subunits. These phenomena suggest the involvement of all individual subunits in amyloid fibril formation of  $\beta$ -conglycinin, accompanied by cooperation with each other.

In the initial stage of heating, DLS results showed that the scattering intensity gradually decreased due to protein hydrolysis upon heating (Figure 3). However, no lag phase was simultaneously found in the formation of amyloid structure in this stage, a precursor of macroscopic fibrils, as evidenced by CD and Th T data (Figures 4 and 5). Correspondingly, in all cases, this fibrillar process is accompanied by progressive polypeptide hydrolysis (Figure 2). These findings suggest that protein hydrolysis may be a requisite step for amyloid-like fibril assembly. Recently, protein hydrolysis has also been observed in the fibril formation of other proteins, including lysozyme,<sup>14</sup>  $\beta$ -lactoglobulin,<sup>11–15</sup> and glycinin.<sup>20</sup> Besides, during the later stage of amyloid fibril formation (12–20 h), the disruption of amyloid ordered structure was observed due to further hydrolysis of the peptides. Taking all results together, the formation of amyloid fibrils of  $\beta$ -conglycinin is considered to follow multiple steps involving protein hydrolysis, assembly to amyloid-like fibrils, and growth into macroscopic fibrils with reorganization of amyloid-like structure.

It is noteworthy that the growth kinetics of the aggregate process and the morphology of formed fibrils considerably varied among various subunits, suggesting the different roles or pathways involved in amyloid fibril formation. Because of the distinct hydrolysis behaviors among the three subunits, including hydrolysis rates and cleavage sites, these phenomena not only suggest a close relationship between the polypeptide hydrolysis and the kinetics of amyloid fibril formation but also confirm that the amino acid composition and sequence of peptides affect the formation of amyloid structure. This is consistent with the previous viewpoint on  $\beta$ -lactoglobulin fibril formation.<sup>11,15</sup>

The  $\alpha$  and  $\alpha'$  subunits exhibited remarkable differences in polypeptide hydrolysis (Figure 2). Interestingly, in terms of amyloid traits, the  $\alpha'$  subunit showed the highest capacity and the fastest rate during formation of amyloid-like structure, and, oppositely, the  $\alpha$  subunit had the lowest capacity and the slowest rate (Figures 4 and 5). In view of the high absolute homologies (90%) between the core regions of the  $\alpha$  and  $\alpha'$  subunits, these observations indicate that the disruption of the  $\alpha$  and  $\alpha'$  subunits, particularly their extension region, may play an important role in affecting the rate of structural changes in fibril formation. Work on the identification of peptide sequences hydrolyzed from

$\beta$ -conglycinin is in progress to disentangle further steps during amyloid fibril formation.

## AUTHOR INFORMATION

### Corresponding Author

\*Phone: (086) 20-87114262. Fax: (086) 20-87114263. E-mail: fexqyang@scut.edu.cn.

### Funding Sources

This research was supported by grants from the Chinese National Natural Science Foundation (Serial No. 21076087).

## ACKNOWLEDGMENT

We thank Dr. Chang-Sheng Wang and Dr. Li-Ya Liu for technical assistance.

## REFERENCES

- (1) Van der Linden, E.; Venema, P. Self-assembly and aggregation of proteins. *Curr. Opin. Colloid Interface Sci.* **2007**, *12*, 158–165.
- (2) Humblet-Hua, K. N. P.; Schellens, G.; Van der Linden, E.; Sagis, L. M. C. Encapsulation systems based on ovalbumin fibrils and high methoxyl pectin. *Food Hydrocolloids* **2011**, *25*, 307–314.
- (3) Rossier-Miranda, F. J.; Schroen, K.; Boom, R. Mechanical characterization and pH response of fibril-reinforced microcapsules prepared by layer-by-layer adsorption. *Langmuir* **2010**, *26*, 19106–19113.
- (4) MacPhee, C. E.; Dobson, C. M. Formation of mixed fibrils demonstrates the generic nature and potential utility of amyloid nanostructures. *J. Am. Chem. Soc.* **2000**, *122*, 12707–12713.
- (5) Arnaudov, L. N.; De Vries, R.; Ippel, H.; Van Mierlo, C. P. M. Multiple steps during the formation of  $\beta$ -lactoglobulin fibrils. *Biomacromolecules* **2003**, *4*, 1614–1622.
- (6) Akkermans, C.; Van der Goot, J. A.; Venema, P.; Van der Linden, E.; Boom, R. M. Formation of fibrillar whey protein aggregates: Influence of heat and shear treatment, and resulting rheology. *Food Hydrocolloids* **2008**, *22*, 1315–1325.
- (7) Giurleo, J. T.; He, X.; Talaga, D. S.  $\beta$ -Lactoglobulin assembles into amyloid through sequential aggregated intermediates. *J. Mol. Biol.* **2008**, *381*, 1332–1348.
- (8) Leonil, J.; Henry, G.; Jouanneau, D.; Delage, M.; Forge, V.; Putaux, J. Kinetics of fibril formation of bovine  $\kappa$ -casein indicate a conformational rearrangement as a critical step in the process. *J. Mol. Biol.* **2008**, *381*, 1267–1280.
- (9) Kroes-Nijboer, A.; Venema, P.; Bouman, J.; Van der Linden, E. The critical aggregation concentration of  $\beta$ -lactoglobulin-based fibril formation. *Food Biophys.* **2009**, *4*, 59–63.
- (10) Arnaudov, L. N.; De Vries, R. Strong impact of ionic strength on the kinetics of fibrillar aggregation of bovine  $\beta$ -lactoglobulin. *Biomacromolecules* **2006**, *7*, 3490–3498.
- (11) Akkermans, C.; Venema, P.; Van der Goot, J. A.; Gruppen, H.; Bakx, E. J.; Boom, R. M.; Van der Linden, E. Peptides are building blocks of heat-induced fibrillar protein aggregates of  $\beta$ -lactoglobulin formed at pH 2. *Biomacromolecules* **2008**, *9*, 1474–1479.
- (12) Oboroceanu, D.; Wang, L.; Brodkorb, A.; Magner, E.; Auty, M. A. E. Characterization of  $\beta$ -lactoglobulin fibrillar assembly using atomic force microscopy, polyacrylamide gel electrophoresis, and in situ fourier transform infrared spectroscopy. *J. Agric. Food Chem.* **2010**, *58*, 3667–3673.
- (13) Bateman, L.; Ye, A.; Singh, H. In vitro digestion of  $\beta$ -lactoglobulin fibrils formed by heat treatment at low pH. *J. Agric. Food Chem.* **2010**, *58*, 9800–9808.
- (14) Lara, C.; Adamcik, J.; Jordens, S.; Mezzenga, R. General self-assembly mechanism converting hydrolyzed globular proteins into giant multistranded amyloid ribbons. *Biomacromolecules* **2011**, *12*, 1868–1875.
- (15) Kroes-Nijboer, A.; Venema, P.; Bouman, J.; Van der Linden, E. Influence of protein hydrolysis on the growth kinetics of  $\beta$ -lg fibrils. *Langmuir* **2011**, *27*, 5753–5761.

- (16) Goldschmidt, L.; Teng, P. K.; Riek, R.; Eisenberg, D. Identifying the amyloids, proteins capable of forming amyloid-like fibrils. *Proc. Natl Acad. Sci. U.S.A.* **2010**, *107*, 3487–3492.
- (17) Sabate, R.; Espargaro, A.; De Groot, N. S.; Valle-Delgado, J. J.; Fernandez-Busquets, X.; Ventura, S. The role of protein sequence and amino acid composition in amyloid formation: scrambling and backward reading of IAPP amyloid fibrils. *J. Mol. Biol.* **2010**, *404*, 337–352.
- (18) Tang, C. H.; Zhang, Y. H.; Wen, Q. B.; Huang, Q. R. Formation of amyloid fibrils from kidney bean 7S globulin (phaseolin) at pH 2.0. *J. Agric. Food Chem.* **2010**, *58*, 8061–8068.
- (19) Akkermans, C.; Van der Goot, A. J.; Venema, P.; Gruppen, H.; Vereijken, J. M.; Van der Linden, E.; Boom, R. M. Micrometer-sized fibrillar protein aggregates from soy glycinin and soy protein isolate. *J. Agric. Food Chem.* **2007**, *55*, 9877–9882.
- (20) Tang, C. H.; Wang, C. S. Formation and characterization of amyloid fibrils from soy  $\beta$ -conglycinin and glycinin. *J. Agric. Food Chem.* **2010**, *58*, 11058–11066.
- (21) Maruyama, N.; Katsube, T.; Wada, Y.; Oh, M. H.; De la Rosa, A. P. B.; Okuda, E.; Nakagawa, S.; Utsumi, S. The roles of the N-linked glycans and extension regions of soybean  $\beta$ -conglycinin in folding, assembly and structural features. *Eur. J. Biochem.* **1998**, *258*, 854–862.
- (22) Yuan, D. B.; Min, W.; Yang, X. Q.; Tang, C. H.; Huang, K. L.; Guo, J.; Wang, J. M.; Wu, N. N.; Zheng, H. G.; Qi, J. R. An improved isolation method of soy  $\beta$ -conglycinin subunits and their characterization. *J. Am. Oil Chem. Soc.* **2010**, *87*, 997–1004.
- (23) Nagano, T.; Hirotsuka, M.; Mori, H.; Kohyama, K.; Nishinari, K. Dynamic viscoelastic study on the gelation of 7S globulin from soybean. *J. Agric. Food Chem.* **1992**, *40*, 941–944.
- (24) Lowry, O. H.; Rosenbrough, H. J.; Lewis, A.; Randall, R. J. Protein measurement with the Folin phenol reagent. *J. Biol. Chem.* **1951**, *193*, 265–275.
- (25) Laemmli, U. K. Cleavage of structural proteins during the assembly of the head of bacteriophage T4. *Nature* **1970**, *227*, 680–685.
- (26) Grudzielanek, S.; Velkova, A.; Shukla, A.; Smirnovas, V.; Tatarek-Nossol, M.; Rehage, H.; Kapurniotu, A.; Winter, R. Cytotoxicity of insulin within its self-assembly and amyloidogenic pathways. *J. Mol. Biol.* **2007**, *370*, 372–384.
- (27) Nilsson, M. R. Techniques to study amyloid fibril formation in vitro. *Methods* **2004**, *34*, 151–160.
- (28) Plakoutsi, G.; Bemporad, F.; Calamai, M.; Taddei, N.; Dobson, C. M.; Chiti, F. Evidence for a mechanism of amyloid formation involving molecular reorganisation within native-like precursor aggregates. *J. Mol. Biol.* **2005**, *351*, 910–922.
- (29) Inglis, A. S. Cleavage at aspartic acid. *Methods Enzymol.* **1983**, *91*, 324–332.
- (30) Lomakin, A.; Benedek, G. B.; Teplow, D. B. Monitoring protein assembly using quasielastic light scattering microscopy. *Methods Enzymol.* **1999**, *309*, 429–459.
- (31) Minor, D. L.; Kim, P. S. Measurement of the  $\beta$ -sheet-forming propensities of amino acids. *Nature* **1994**, *367*, 660–663.
- (32) Mishra, R.; Sorgjerd, K.; Nystrom, S.; Nordigarden, A.; Yu, Y. C.; Hammarstrom, P. Lysozyme amyloidogenesis is accelerated by specific nicking and fragmentation but decelerated by intact protein binding and conversion. *J. Mol. Biol.* **2007**, *366*, 1029–1044.